Geometric decorrelation in acoustic tools for surveying the seafloor

Pierre Cervenka

Geometric decorrelation in acoustic tools for surveying the seafloor

P. Cervenka

CNRS UMR 7190, UPMC (P6) Institut Jean le Rond d'Alembert, 2, place de la gare de ceinture, 78210 Saint-Cyr-L'Ecole, France
pierre.cervenka@upmc.fr

Geometric decorrelation, also known as baseline decorrelation, is a limiting factor in the performance of interferometers that feature large baselines. This phenomenon can be thus a bottle-neck in the development of new surveying tools, e.g. forward-looking synthetic interferometers or imaging systems based on squint synthetic aperture. The mechanism responsible for geometric decorrelation is put in evidence by using a simple model of surface scattering, with an idealized pair of transmitter-receiver running the 'stop and hop' scenario within a 2D geometry. Geometric decorrelation can be countered in several cases of practical interest. The choice of the transmitted signals and the relevant signal processing at receive that aim at reducing or even cancelling this effect are developed. Numerical examples are given in realistic configurations.

1 Introduction

Finding the direction of arrival of echoes to determine the topography of the seafloor with an acoustical interferometer is based on the correlation between echoes that are received from the scene at different locations of the physical or synthetic antenna. Because the scenes of interest are 2D surfaces, the received echoes are closely related to the convolution of the projection of the transmitted waves on the bottom with the impulse response of the bottom swept under particular angles of view. The correlation of the echoes that originate from the same bottom area but seen under different grazing angles contributions may be altered by the so-called baseline or geometric decorrelation, and its detrimental effect increases with the width of the baseline.

Interferometric side-scan sonar systems, including synthetic aperture sonars (SAS) [1], collect data by insonifying the seafloor athwartships within a large fan in the across-track plane, and use at least two receiving antennas on each side of the platform to derive bathymetry. Forward-looking systems can also be used to produce seafloor mapping. Although the realization of split-beam sonar technology has been foreseen long ago [2], it seems that the only experimental prototype, COSMOS, based on a forward-looking interferometric receiver [3], has actually been operated at sea. All these interferometers feature ultrashort or short baselines. Another interesting way to implement the interferometric principle is to process the signals obtained at distinct locations of a single echographic system. The concept has been proposed by Li and Goldstein [4] in the spaceborne synthetic aperture radar (SAR) domain: the interferometric configuration is achieved with a conventional SAR system, which is flown on a platform in a nearly repeat ground-track orbit [5]. Now, such a side-looking multipass concept is not applied in the underwater domain. However, it suggests another kind of synthetic interferometer that could be investigated for seafloor mapping. The idea would be to take advantage of the successive views obtained with a forward-looking system, such as a gap filler with a single receiving array: bathymetry would be derived by correlating the complex images obtained from successive pings. The key challenge is to overcome the severe constraint raised by geometric decorrelation with such forward-looking sonars.

Baseline decorrelation has been addressed for a long time in the SAR community (e.g., [6][7][8][9][10]) because interferometric SAR systems currently feature large baselines. Interferometric SAR in the presence of squint is also specifically studied e.g., in [11]. Although the basis of baseline decorrelation has not been completely neglected in the underwater acoustics domain (e.g., [12][13]), experience shows that the phenomenon and its consequences are generally not fully grasped.

The mechanism responsible for baseline decorrelation is thoroughly addressed in Section 2. One focuses on the correlation coefficient that can be expected at the equivalent of two phase centers in a simplified 2-D model of forward-looking sonar (Fig. 1). The "stop-and-hop" scenario is assumed: the pair transmitter–receiver is modeled by a phase center that is successively located along-track at C_1 and C_2 during two consecutive ping cycles. The random scatterers are uniformly distributed along a straight line in the alongtrack vertical plane. Signal processing and choices of proper reference signals that aim at reducing or canceling baseline decorrelation are analyzed in Section 3.

2 Correlation of the received signals

Baseline decorrelation is dictated the dependency on the roundtrip lengths and on the characteristics of the transmitted signal footprints, of the correlation coefficient $\rho = \langle s_1 s_2^* \rangle / \sqrt{\langle s_1 s_1^* \rangle \langle s_2 s_2^* \rangle}$ between the echoes (s_1, s_2) received from the seafloor at two different locations.

Geometric notations are presented Fig. 1. The portion of the seafloor under investigation is around M_0. One assumes that $b \ll r$, so that the angle $\phi \approx r^{-1} b \cos\zeta$ is small. Considering a reference transmit signal with a narrow bandwidth, its analytical form $s(t) = A(t)\exp(j\omega_0 t)$ is expressed, after pulse compression if applicable, as the product of a carrier at pulsation ω_0 and a complex modulating envelope $A(t)$ whose bandwidth ω_A is narrow, i.e., $B = \omega_A/\omega_0 \ll 1$. The slant range resolution is related to the frequencies and the carrier wavelength λ_0 through $\Delta r \equiv \lambda_0/(2B)$. The ground range resolution $\Delta x = \Delta r/\sin\gamma$ is the length of the echographic footprint of the signal on the seafloor. It can be assumed that $\Delta x \ll r$, so that the angle $\psi_{\Delta x} = r^{-1}\Delta x \cos\gamma$ is small either.

Referencing the timing of the signals at ping transmits, the contribution to the signal received by C_i at time t from a target M_x after the roundtrip distance $d_i(x) = 2C_iM_x$ is

$$s_i\left(t, d_i(x)\right) = w(x)\, s\left(t - d_i(x)/c\right), \qquad (1)$$

where $w(x)$ is the complex response of the scatterer M_x (c denotes the sound speed in water) We are looking at the signals received in C_1 and C_2 at the times $t_a = t_1$ and $t_b = t_2 + \delta_t$ respectively, where $t_i = c^{-1} d_i(0)$ denotes the roundtrip delays between C_i and M_0. The time difference $t_1 - t_2$ so introduced in $t_a - t_b$ is meant to co-register the pieces of floor that are seen by the receivers. The additional time lag δ_t may be caused for example by lack of knowledge about the relative direction ζ of the ground. Summing over the contributions of all scattering points, the received signal samples read:

$$s_1(t_a) = \int s_1\left(t_a, d_1(x)\right)\mathrm{d}x, \;\; s_2(t_b) = \int s_2\left(t_b, d_2(x)\right)\mathrm{d}x \qquad (2)$$

Several instances of the calculation of the expected value of the complex cross-correlation $\langle s_1(t_a)s_2^*(t_b)\rangle$, where specific narrow bandwidth envelops A are considered (usually a boxcar), can be found in the literature (e.g., [4], [6], [7], and [12]). However, the scatterers being assumed random, uncorrelated and uniformly distributed, the normalized cross-correlation factor can take the following synthetic form that applies also with wide-band signals:

$$\rho_\beta(\delta_t) = \langle s_1 s_2^* \rangle \Big/ \sqrt{\langle s_1 s_1^* \rangle \langle s_2 s_2^* \rangle} = \chi_s(\delta_t, \beta) \big/ \chi_s(0,0), \quad (3)$$

with $$\chi_s(\delta_t, \beta) = \int_{-\infty}^{\infty} s(t)\, s^*\big((1-\beta)t + \delta_t\big)\,\mathrm{d}t \quad (4)$$

and $$\beta = \phi / \tan\gamma = b\cos\zeta \big/ (r\tan\gamma) \ll 1. \quad (5)$$

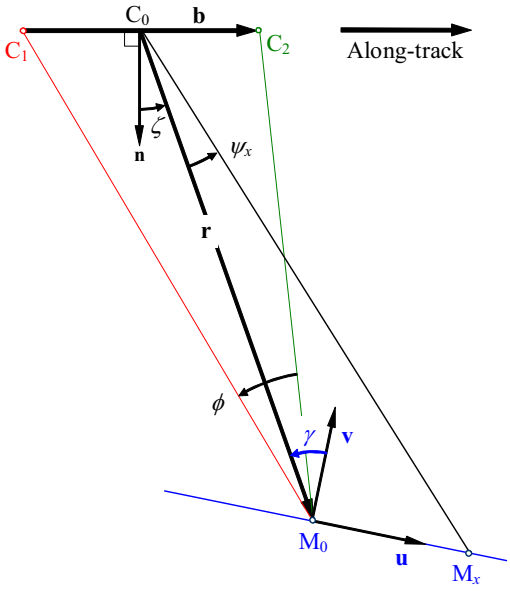

Figure 1. Modeled phase centers (C_1,C_2) and seafloor (M_x). C_0: mid-point of segment C_1C_2; **n**, **u**, **v**: unit vectors. Length b is exaggerated compared to the scale given by r.

Eq. (4) is the wideband version of the ambiguity function, which quantifies the extent to which the signal s is similar to itself, delayed by δ_t, and stretched by the relative ratio β. Hence, the loss of coherence between s_1 and s_2 proceeds from two effects, which the parameters δ_t and β quantify. The first is caused by the mismatch of the footprints that are compared. The better the delay between the signals to be compared is adjusted ($\delta_t \to 0$), the more this contribution to the decorrelation is reduced. The complete lack of delay compensation amounts to process straightforwardly synchronous signals, i.e., with $t_a = t_b$. The footprint shift is then $\delta_x = b\sin\zeta / \sin\gamma$. This problem has been thoroughly described and studied (e.g., in [13], [14], and [15]).

Concerning the second effect, let us consider a null time lag ($\delta_t = 0$); this means that the delay $t_a - t_b$ is such that the contributions from the scatterer located at M_0 are the same for both signal samples s_1 and s_2. However, the contributions from scatterers located at M($x\neq0$) come from parts of the reference signal that differ by the time shift $\tau \approx \beta t_i$. This is the key to baseline decorrelation, sometimes also called geometric decorrelation. Because of the slight angular difference ϕ, the scene of scatterers around M_0 is viewed from C_2 at a smaller incidence angle than from C_1. Consequently, the scene viewed from C_2 is compressed in range compared to the scene viewed from C_1. This explains why the impulse response of the bottom viewed by C_2 is the same as that viewed by C_1 but at a faster rate, which induces an expansion of the spectrum of this response towards higher frequencies. The relative time stretching is equal to the relative variation in the range interval, which is in fact quantified by β (Fig. 2), i.e., MA/MB ≈ 1+β. As stressed in [8], this does not mean that the signal received in C_2 is shifted in frequency compared to the one in C_1. It just means that the components of the floor reflectivity spectrum found in the first signal are transformed in the second spectrum by the affinity whose relative ratio is β. It also implies that the information about the floor reflectivity shared by the signals s_1 and s_2 includes neither the lower part of the spectrum of s_2 nor the upper part of the spectrum of s_1.

Taking into account the narrow bandwidth of the reference signal, the coefficient (3) reduces into:

$$\rho_\beta(\delta_t) = \exp(-j\omega_0\delta_t)\, \chi_A(\delta_t, \beta\omega_0) \big/ \chi_A(0,0), \quad (6)$$

with $$\chi_A(\delta_t, \beta\omega_0) = \int_{-\infty}^{\infty} A(t)\, A^*(t+\delta_t) \exp(j\beta\omega_0 t)\,\mathrm{d}t \quad (7)$$

The product $\omega_0\delta_t$ is the classical differential phase remaining after the delay compensation $t_a - t_b$; $\chi_A(\delta_t,\delta_\omega)$ is the ambiguity function of the narrowband signal A computed for the time and frequency shifts δ_t and δ_ω, respectively.

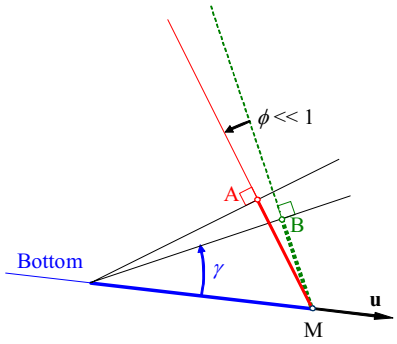

Figure 2. The wavefront perpendicular to AM takes a longer time than the one perpendicular to BM to sweep the same part of the seafloor.

The magnitude of the baseline decorrelation is dictated by the phase excursion $\varphi_{\max}$ that occurs in the exponential term of (7) between the effective time limits of integration, i.e.,

$$\varphi_{\max} \approx \left[\delta_\omega t\right]_{-T/2}^{+T/2} = \beta\omega_0 T = 2\pi\beta B^{-1} = 2\pi\phi \big/ (B\tan\gamma). \quad (8)$$

where $T \equiv 2\pi\omega_A^{-1}$. The coherence is likely to be lost if $\varphi_{\max} \approx 2\pi$, i.e.,

$$(r\phi)(\psi_{\Delta x}/\lambda_0) \equiv 1/2 \quad \Leftrightarrow \quad \beta B^{-1} = \phi \big/ (B\tan\gamma) \equiv 1. \quad (9)$$

Eq. (8) shows that the baseline decorrelation is inversely proportional to the relative bandwidth B. Eq. (9) states a very simple rule: the coherence is entirely lost when the relative bandwidth B is equal to β, i.e., when the floor re-

flectivity spectrum embedded in the signals s_1 and s_2 has shifted between them by more than the bandwidth of the reference signal: the signals no longer share any common information about the seafloor. There is also an equivalent, intuitive interpretation of (9). Let us consider an interferometer whose baseline is $r\phi$, and a target that departs from boresight by a small angle ψ_x. The differential phase of the signals that the interferometer receives from this target is $\varphi_x \approx r\phi \times \psi_x/\lambda_0$. With a scene of uniformly distributed scatterers that is wide enough for the differential phase contributions of each of them to be spread over 2π, the overall coherence of the received signals vanishes. In a more general approach, the first formulation in (8) and (9) exhibits the direct link with the Van Cittert–Zernike theorem [16], which states that for incoherent noise sources the spatial correlation function of the radiated noise is the Fourier transform of the illumination function. In the far field of the signal footprint, a way to make this point is that the coherence is lost whenever the lateral distance $r\phi$ between the points of observation is of the order of the length $\lambda_0/\psi_{\Delta x}$ of a transmitter that would illuminate from the same area a scene of uncorrelated scatterers at the angular frequency ω_0, (hence over an aperture $\psi_{\Delta x}$).

From a practical point of view, the correlation between the signals received at C_1 and C_2 is searched by integrating over an interval of time Δt. The analytical development to derive the corresponding correlation coefficient is quite similar to the arguments that led to (6). One finds

$$\rho(\delta_t, \Delta t) = \rho_\beta(\delta_t)\,\mathrm{sinc}(\beta\omega_0\Delta t/2). \qquad (10)$$

The cardinal sinus factor in (10) (whose argument reads also $B^{-1}\beta\omega_4\Delta t/2$) can be significantly smaller than unity because the relative bandwidth B is small compared to unity. Hence integrating directly the complex conjugate signals received by the interferometer over an interval of time Δt may reduce the coherence because the mismatch in the signal footprints grows with the distance from M_0 during integration. However, this effect can be countered as is shown next.

3 Reduction of baseline decorrelation

3.1 Matching signals before integration

It has been pointed out already that the difference between the points of view from C_1 and C_2 induces a relative time stretching in the corresponding impulse responses from the floor. This suggests a simple method to avoid the losses shown in (10). The procedure is known in the InSAR literature as wavenumber (or spectral) shift filtering [8]. It consists of shifting the central frequency of the signals before evaluating the cross products. In practice, this is done by introducing a corrective factor $\exp\left(j\tilde{\beta}\omega_0 t\right)$ in the complex product being integrated. Doing so, (10) becomes

$$\tilde{\rho}(\delta_t, \Delta t) = \rho_\beta(\delta_t)\,\mathrm{sinc}\left(\left(\beta - \tilde{\beta}\right)\omega_0\Delta t/2\right) \qquad (11)$$

The meaning of this operation can be easily understood: the main direction of the incoming echoes $\zeta(t)$ changes with time, so that the instantaneous differential phase of the complex conjugated product rotates along the interval of integration. The corrective factor is introduced to compensate for this shift of the differential phases. The spectrum of the reference signal s is definitively embedded in the spectrum of the seafloor response, the latter being shifted in building s_2 compared to s_1. The operation described above aligns these seafloor responses. The spectrum of the reference signal which frames s_1 and s_2 is shifted in opposite directions prior to the integration of their conjugate products; hence, the irreducible character of the decorrelation expressed by ρ_β (6). Nevertheless, matching the impulse response spectra of the floor allows integrating over a time interval Δt without increasing the loss in coherence.

Widening the interval of integration is convenient for performing the phase unwrapping when the baseline is large enough to give rise to ambiguities. Each swath is processed in two successive steps: a large interval of integration is chosen in the first step, resulting in a smooth and slow evolution of the differential phase. The range resolution is degraded, but due to the continuity and slow evolution of the phase, the unfolding is more reliable because of the averaging effect that is so enabled. The second step is performed with a smaller interval of integration, thereby improving the horizontal resolution of the bathymetry. The phases that are found in the first pass are used as references in the second step $\left(\left|\varphi - \tilde{\varphi}\right| < \pi\right)$. This technique has been used with the COSMOS forward looking sonar [3], whose baseline has the length of two wavelengths. In this process, the smoothed version of the bathymetry given by the previous ping is used to derive the evolution of the parameter $\beta(t)$ applied to flatten the phase of the current ping [17][18]. It is likely that some commercial software uses a similar type of process, although the direct link with baseline decorrelation is not necessarily recognized.

3.2 Using two distinct reference signals

There is a radical method to counter the baseline decorrelation in the bistatic configuration. It consists of sending from C_1 and C_2 two distinct signals, the difference being the time rate whose relative factor $\overline{\beta}$ is close to a targeted value β. This is the principle of the tunable interferometric SAR devised in [8] for multipass systems.

$$s_{(1)}(t) = s(t),\ \ s_{(2)}(t) = s\left(\left(1+\overline{\beta}\right)t\right) \qquad (12)$$

The introduction of the relative timescale factor $\overline{\beta}$ modifies the coherence (6), which now becomes

$$\overline{\rho_\beta}(\delta_t) = \rho_{\beta-\overline{\beta}}(\delta_t) \qquad (13)$$

The decorrelation can be entirely cancelled if $\overline{\beta} = \beta$ (with $\delta_t = 0$), i.e., by modifying only the carrier frequency ω_0 of the second transmitted signal by the ratio $(1+\beta)$.

The integration of the conjugate products of the received signals over a time interval Δt must be also compensated to match the spectra of the floor response in both received signals. The correlation coefficient reads:

$$\tilde{\overline{\rho}}(\delta_t, \Delta t) \approx \rho_{\beta-\overline{\beta}}(\delta_t)\,\mathrm{sinc}\left(\left(\beta - \tilde{\beta}\right)\omega_0\Delta t/2\right) \qquad (14)$$

The compensation is applied at a post-processing stage. Consequently, the parameter $\widetilde{\beta}$ can be adjusted to compensate the geometry factor β as well as possible corresponding to the area around which the integration is performed. Consequently, the technique of changing the signal used between successive pings can be then tuned with $\overline{\beta} = \beta$ to cancel entirely the geometric decorrelation.

However, this latter compensation is effective only over a limited part of the swath because the parameter $\overline{\beta}$ is a constant whereas β is not. In order to illustrate the extent of the domain for which the method may apply, one considers a boxcar modulating envelope A. Eq. (14) takes the form

$$\widetilde{\rho} \approx \operatorname{sinc}\left(\left(\beta - \overline{\beta}\right)\omega_0 T/2\right), \tag{15}$$

The floor is assumed to be horizontal so that $\zeta = \gamma$. The interferometer is at the altitude $h = r\cos\gamma$ (Fig. 3). The correlation is equal to unity for the piece of floor seen around the incidence $\overline{\gamma}$, so that $b\cos^3\overline{\gamma}/\left(h\sin\overline{\gamma}\right) = \overline{\beta}$. The width $\Delta\gamma$ of the sector for which the compensation $\overline{\beta}$ yields a significant improvement can be estimated by looking at the limits for which β, and consequently γ, satisfies $\left|\left(\beta - \overline{\beta}\right)\frac{\omega_0 T}{2}\right| < \frac{\pi}{2} \Leftrightarrow \left|\frac{\cos^3\gamma}{\sin\gamma} - \frac{\cos^3\overline{\gamma}}{\sin\overline{\gamma}}\right| < \frac{\pi h}{b\omega_0 T}$. One finds

$$\Delta\gamma \approx Bb^{-1}h\tan^2\overline{\gamma}/\left(1 + 2\sin^2\overline{\gamma}\right). \tag{16}$$

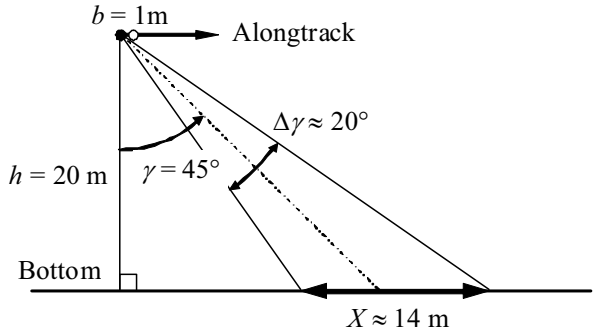

Figure 3. Sector for which correlation is recoverable with a frequency shift ratio $\overline{\beta}$ =1/40 between successive pings

For example, let us consider a forward-looking sonar (e.g., a gap filler) running at the carrier frequency f_0 = 300 kHz and using 10 kHz-bandwidth signals, so that the relative bandwidth is B = 1/30. The system is surveying the ground at the altitude h = 20 m, with a displacement b = 1m between successive pings. Looking around the zone seen with the incidence angle γ = 45°, the baseline decorrelation is determined by the factor β = 1/40. Using the same signal for consecutive pings, the relative bandwidth (B = 1/30) is not large enough compared to β to obtain sufficient correlation between successive signals. If the carrier frequency is shifted by βf_0 = 7.5 kHz between consecutive pings, the correlation is recovered over a sector whose approximate width is $\Delta\gamma \approx 0.5\, Bb^{-1}h$ rad ≈20° (16), equivalent to a horizontal range interval X = 14 m. This horizontal range interval X is much larger than the alongtrack translation b of the platform between successive pings. The vertical site sector scanned by the sonar can thus be limited to the interval $\Delta\gamma$ around γ, still ensuring a complete coverage of the nadir band.

3.3 Enlarged bandwidth and filtering

Because the central frequency cannot be increased indefinitely, a better strategy can be employed to reduce or even cancel the geometric decorrelation in both the synthetic and classical configurations. It consists in transmitting at each ping an identical larger-bandwidth signal, so that the sub-banded parts of this signal, as explained next, mimic the pair of reference signals described in (12).

Let us consider a transmitted signal whose spectrum lies in the interval $[f_a, f_b]$. In order to counter a geometric factor $\overline{\beta}$, the signals received by C_1 and C_2 must be low-pass and high-pass filtered with the cutoff frequencies $\left(1+\overline{\beta}\right)^{-1} f_b$ and $\left(1+\overline{\beta}\right) f_a$, respectively. This is equivalent to dealing with the following pair of transmitted signals:

$$\begin{cases} s_{(1)}(t) = s\left[f_a,\ \left(1+\overline{\beta}\right)^{-1} f_b\right] \\ s_{(2)}(t) = s\left[\left(1+\overline{\beta}\right) f_a,\ f_b\right] \end{cases} \tag{17}$$

where $s[f_{\min}, f_{\max}]$ denotes the filtered version of s in the given interval. The trick consists in that the signal s has to be chosen so as the filtered parts (17) comply as much as possible to the reference signals (12). The integration over the time interval Δt is then performed after shifting the spectra of the received signals as described previously, with the same ratio $\widetilde{\beta} = \overline{\beta}$ (Fig. 4). The relevant parts of the impulse response of the seafloor are thus realigned. From a practical point of view, the filtering and spectral shifting of the pieces of received signals can be done in a single operation. The geometric factor β being range-dependent, the technique can be implemented as an adaptive process in which the shift factor is adjusted along the swath (e.g., [19][20]). The maximal correlation that may be expected, finally, is dictated by how much the sub-band filtered versions (17) of the reference s indeed comply with the equivalent of (12). Hence, the most desirable signal s would be such that regardless of the value of β ($\ll 1$), we have

$$s_{(1)}(t) = s_{(2)}\left((1-\beta)t\right), \tag{18}$$

where $s_{(i)}$ is defined by (17). An example of a good candidate for the implementation of this procedure is the linear frequency modulated chirp. Let us consider such a transmitted signal c_0 whose central angular frequency, relative bandwidth, and duration are ω_0, B and T_0, respectively. B must be larger than the parameter β that characterizes the geometric configuration of the zone to be analyzed. Pulse compression and filtering of the respective signals received by C_1 and C_2 are performed in the same operation by using the chirp references c_1 and c_2 that are properly truncated versions of c_0 so that the instantaneous frequencies of c_2 is continuously upshifted by the ratio $(1+\beta)$ relatively to the instantaneous frequency of c_1 (Fig. 5). The following resulting equivalent reference signals (17) come close to the desired property (18):

$$\begin{cases} s_{(1)(\beta)}(\tau) = \int c_0(t)\, c^*_{1(\beta)}(t+\tau)\,\mathrm{d}t \\ s_{(2)(\beta)}(\tau) = \int c_0(t)\, c^*_{2(\beta)}(t+\tau)\,\mathrm{d}t \end{cases} \quad (19)$$

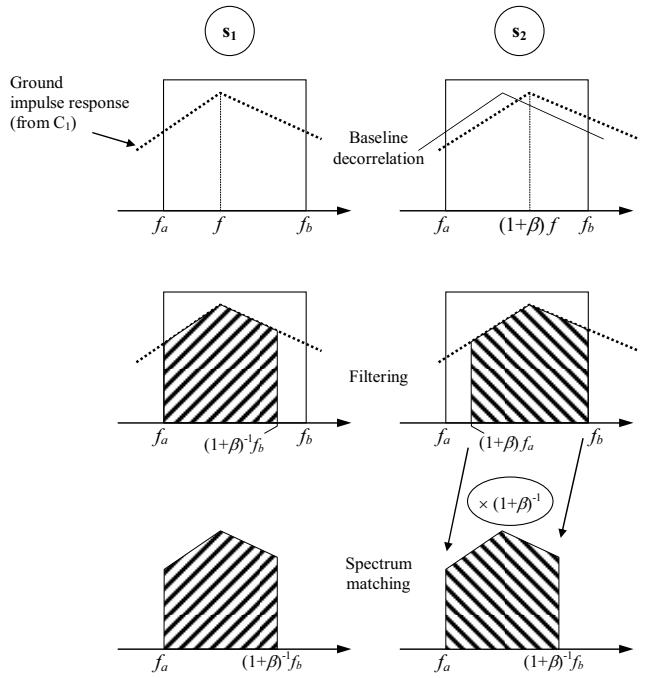

Figure 4. Schematic representation of the spectra. Upper part: recorded signals; middle and lower parts: processing scheme before evaluating the cross products and performing the integration.

The maximal correlation factor that can be expected is the peak of the cross-correlation calculated with the proper rescaling, i.e., $\tilde{\rho}_{c_0}(\beta) = \max\left|\tilde{\eta}_{c_0,\beta}(\tau)\right|$ with

$$\tilde{\eta}_{c_0,\beta}(\tau) = \frac{\int s_{(1)(\beta)}(t)\, s^*_{(2)(\beta)}\left((1+\beta)^{-1}(t+\tau)\right)\mathrm{d}t}{\sqrt{\left(\int\left|s_{(1)(\beta)}\right|^2 \mathrm{d}t\right)\left((1+\beta)\int\left|s_{(2)(\beta)}\right|^2 \mathrm{d}t\right)}} \quad (20)$$

In addition, the -3 dB width $\widetilde{\Delta\tau}(\beta)$ of the envelope of the function $\tilde{\eta}_{c_0,\beta}(\tau)$ gives the evolution of the slant range resolution at the output of the cross-correlation. The interest of this process becomes evident if we compare the expected performances given by $\tilde{\rho}_{c_0}$ and $\widetilde{\Delta\tau}$ with the values ρ_{c_0} and $\Delta\tau$ obtained when the time is not rescaled, i.e., with:

$$\eta_{c_0,\beta}(\tau) = \frac{\int s_{(1)(\beta)}(t)\, s^*_{(2)(\beta)}(t+\tau)\,\mathrm{d}t}{\sqrt{\left(\int\left|s_{(1)(\beta)}\right|^2 \mathrm{d}t\right)\left(\int\left|s_{(2)(\beta)}\right|^2 \mathrm{d}t\right)}}. \quad (21)$$

The complete process clearly performs better than what can be expected from only filtering the received signals (Figs. 6-7). In the latter case, the correlation is so poor beyond $\beta = 0.4\,B$ that the time resolution of the cross-correlated signals no longer has any meaning. Matching the spectra makes it possible to keep 90% of the correlation even if the baseline factor reaches 80% of the transmitted signal bandwidth. On the other hand, this result is obtained at the expense of a deteriorating range resolution. The central part of the envelope of a compressed chirp signal with frequency bandwidth F_i being consistently modeled by $\mathrm{sinc}(\pi F_i t)$, an approximation of the time resolution is simply $\Delta t_{-3dB} \approx 0.9\, F_i^{-1}$. The relative bandwidth B_i of the signals that yields correlation in the interferometer is reduced by β compared to the full bandwidth B of the transmitted signal, i.e., $B_i \approx B - \beta$, so that the degraded resolution reads in the dimensionless unit scaled by the initial frequency bandwidth F_0:

$$F_0 \Delta t_{-3dB} \approx 0.9\, F_i^{-1} F_0 \approx 0.9\left(1 - \beta/B\right)^{-1}. \quad (22)$$

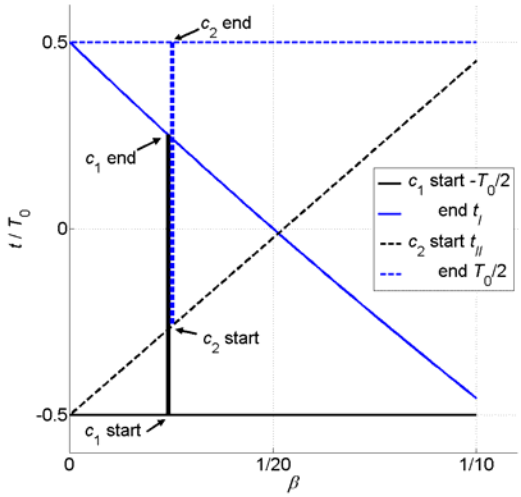

Figure 5. Dependency with β of the limits of the chirp signals, ($B = 0.1$, illustration with $\beta \approx 1/40$). Because $\beta \ll 1$, the time boundaries are closely approximated by linear laws, i.e. $t_{1\,\max} \approx -t_{2\,\min} \approx (1\text{-}2\beta B^{-1})T_0/2$, although it can be noticed that these curves do not cross exactly at $t = 0$ when $\beta = B/2$.

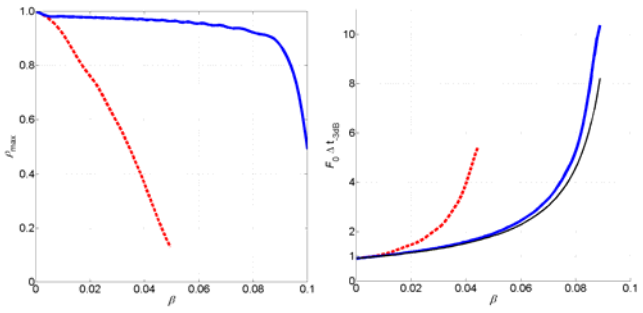

Figure 6. Dependency on the baseline factor β, with an LFM chirp ($B = 0.1$, $F_0T_0 = 90$) of: left: the maximal expected correlation (solid line: with time scaling (20); dashed line: without time scaling (21)); right: the dimensionless time resolution $F_0\Delta t_{-3\mathrm{dB}}$ of the interferometer (bold blue solid line: with time scaling, i.e., width of $\tilde{\eta}$ (20); thin black solid line: approximate relation (22); red dashed line: without time scaling, i.e., width of η (21)).

It can be checked in Fig. 7 that the -3 dB width of the envelope of $\tilde{\eta}_{c_0,\beta}$ is closely approximated with (22). This example thus shows that a baseline decorrelation involving a spectral shift that amounts to half the available bandwidth can be compensated for ($\rho > 0.96$) with the only drawback of halving the range resolution.

4 Conclusion

It is established that baseline decorrelation caused by a flat surface consisting of uniformly, uncorrelated scatterers can be simply quantified by the ambiguity function of the transmitted signal. Recognizing that this formulation is a consequence of the stretching of the ground impulse response with change in the incident angle of view, methods to counter the loss of coherence can be straightforwardly devised. Geometric decorrelation is not a Doppler effect. It is simply that the same information about the floor reflectivity is recorded in a higher frequency domain when collected at a smaller incidence angle of view. Hence when processing by cross-correlation signals received from different points of view, it calls for two measures: 1) to select in each signal the part of the frequency spectrum that shares common information about the seafloor; 2) to realign these spectra before performing the cross-correlations. In other words, it amounts to taking care that the projections on the bottom of the transmitted signals associated to each center C_i are identical, and that conversely the received echoes are next properly realigned and stretched so as to fit their respective origin from the bottom. The first part can be done either by applying filters on the received signals, or by transmitting different signals directly with the shifted spectra. The second operation takes place while performing the cross products that are integrated in the resolution cell; this requires the only introduction of a phase shifting term when dealing with narrowband signals. The best achievable result is indeed obtained if the expected echoes yield, after being handled with these processes, two identical replica (18). To this end, using a chirp signal at transmit can be very convenient. However, the simplicity of the underlying idea should not hide the difficulties of the actual implementation. The compensation for misregistration (δ_i) and for geometric decorrelation (β) depends on the a priori knowledge of the bathymetry, which calls for adaptative procedures. In addition, azimuthal rotation of the point of views, surface roughness and volume scattering limit the correlation that can be ultimately achieved.

References

[1] M.P. Hayes, P.T. Gough, Synthetic aperture sonar: a review of current status*, IEEE J. Ocean. Eng.* **34**(3), 207-224, 2009.

[2] W.K. Stewart, Three-Dimensional modeling of seafloor backscatter from sidescan sonar for autonomous classification and navigation, *Proc. 6th Int. Symp. on Unmanned Untethered Submersible Technology*, 372-392, 1989.

[3] P. Cervenka and J. Marchal, Imaging with a new multi-look front-scan sonar system, *Acta Acustica / Acustica* **90** 1, 38-48, 2004.

[4] F.K. Li, R.M. Goldstein, Studies of multibaseline spaceborne interferometric synthetic aperture radars*, IEEE Trans. Geosci. Remote Sens.* **28**(1), 88-97, 1990.

[5] J. Homer, I.D. Longstaff, Z. She, D. Gray, High resolution 3-D imaging via multi-pass SAR*, IEE Proc. Radar Sonar Navig*. **149**(1), 45-50, 2002.

[6] H.A. Zebker, J. Villasenor, Decorrelation in interferometric radar echoes, *IEEE Trans. Geosci. Remote Sens.* **30**(5), 950-959, 1992.

[7] E. Rodriguez, J.M. Martin, Theory and design of interferometric synthetic aperture radars, *IEE Proc-F,* **139**(2), 147-159, 1992

[8] F. Gatelli, A. Monti Guarnieri, F. Parizzi, P. Pasquali, C. Prati, F. Rocca, The wavenumber shift in SAR interferometry*, IEEE Trans. Geosci. Remote Sens.* **32**(4), 855-865, 1994.

[9] R. Bamler, P. Hartl, Synthetic aperture radar interferometry, *Inverse Problems* **14**, R1-R54, 1998.

[10] P.A. Rosen, S. Hensley, I.R. Joughin, F.K. Li, S.N. Madsen, E. Rodríguez, R.M. Goldstein, Synthetic aperture radar interferometry, *Proc. IEEE*, **88**(3), 333-382, 2000.

[11] M. Bara, R. Scheiber, A. Broquetas, A. Moreira, Interferometric SAR signal analysis in the presence of squint, *IEEE Trans. Geosci. Remote Sens.* **38**(5), 2164-2178, 2000.

[12] G. Jin, D. Tang, Uncertainties of differential phase estimation associated with interferometric sonars*, IEEE J. Ocean. Eng.* **21**(1), 53-63, 1996

[13] X. Lurton, Swath bathymetry using phase difference: theoretical analysis of acoustical measurement precision, *IEEE J. Ocean. Eng.* **25**(3), 351-363, 2000.

[14] J.S. Bird, G.K. Mullins, Analysis of swath bathymetry sonar accuracy, *IEEE J. Ocean. Eng.* **30**(2), 372-390, 2005.

[15] C. Sintes, G. Llort-Pujol, D. Guériot, Coherent probabilistic error model for interferometric sidescan sonars, *IEEE J. Ocean. Eng.* **35**(2), 412-423, 2010.

[16] J.W. Goodman, Statistical Optics. New York: Wiley-Interscience, 1985.

[17] P. Cervenka, Characterization and observation of the seafloor with a new multibeam front-scan sonar system, *Final reports* on Tasks 4.1 (Data Alignment – Imaging), and 4.2 (Interferometry – Bathymetry), European Mast III programme, contract n° MAS3-CT97-0090 (DG 12 – ESCY).

[18] P. Cervenka, J. Marchal, P. Janvrin, An interferometric front scan sonar system : Benefits in compound imaging and estimate of the relief ahead of the platform afforded by the interferometric capability, *Proc. 5th European Conference on Underwater Acoustics* (ECUA 2000), Vol. I, 343-348, 10-13 July 2000, Lyon.

[19] A. Reigber, Range dependent spectral filtering to minimize the baseline decorrelation in airborne SAR interferometry, *IEEE Int. Geosci. and Remote Sens. Symp.* (IGARSS'99), Proc. vol. **3**, 1721-1723, 1999.

[20] T.O. Saebo, R.E. Hansen, H.J. Callow, B. Kjellesvig, Using the cross-ambiguity function for improving sidelooking sonar height estimation, *Underwater Acoustic Measurements :Technologies & Results, 2nd Int. Conference & Exhibition*, Heraklion, Crete, Greece, 25-29 June 2007.